

# A combined optical and magneto-optical measurement system

W. J. M. A. Geerts, J. C. Lodder, and Th. J. A. Popma

MESA Research Institute, University of Twente, P.O. Box 217, 7500 AE Enschede, The Netherlands

(Received 10 July 1991; accepted for publication 9 October 1991)

A magneto-optical (MO) Kerr tracer based on an ellipsometer was developed for studying the surface magnetic properties of thin films. This system can be used to measure the optical properties  $n$  and  $k$ , which are strongly related to the magneto-optical parameters  $\theta_k$  and  $\eta_k$ . In order to carry out measurements on materials having a small  $\theta_k$  we have developed a multiple reflection sample holder which gives an enhancement of the rotation. The behavior of the sample holder is explained in terms of Jones matrices. The optical and magneto-optical properties for a thickness series of Co-Cr films were measured. Comparative measurements on other systems gave similar results.

## I. INTRODUCTION

The application of thin magnetic films for high-density recording media is most promising. The small head-to-medium distance, as well as the decreasing layer thickness, both "a must" to obtain high information densities, are responsible for enhanced interest in the surface of present-day recording materials. As the higher frequencies are only written in the top layer<sup>1</sup> and the stray field, which is so important in the reading process, can be largely influenced by the magnetic state of the surface layer,<sup>2</sup> it is clear that it is of great importance to know and understand the magnetic behavior at the air interface of the recording medium. An interesting region in this context is the depth over which the chemical, structural, morphology, and magnetic properties differ from those of the bulk parameters (typically about 4 to 40 nm for rf sputtered Co-Cr films).<sup>2,3</sup>

Several techniques, based on different physical quantities, have been proposed in order to study the surface magnetism. Under the assumption that the magnetic stray field is largely influenced by the film's upper part, Bitter techniques<sup>4</sup> or magnetic force microscopy<sup>5</sup> are suitable tools. Study of the spins of the secondary electrons in a scanning electron microscope (SEM) provides surface sensitive information because of the filter function of the top atom layers.<sup>6</sup> A very elegant method to study the surface magnetism is the magneto-optical measurement method. This method is based on the difference in adsorption of right circular (RCP) and left circular polarized (LCP) light<sup>12</sup> which is induced by the combination of spin-orbit interaction and exchange coupling.<sup>7</sup> In the case of transition metals the penetration depth of visible light is limited by the high adsorption [around 20 nm for Co-Cr (19-at. % Cr) at  $\lambda = 630$  nm], which makes the magneto-optical measurement technique also surface sensitive.

The Kerr rotation  $\theta_k$  is an extrinsic material parameter.<sup>8</sup> For this reason the study of the MO parameters has to be accompanied by the study of the optical parameters in order to be able to explain the results. In this paper a description of a Kerr tracer/ellipsometer built in our laboratory is presented. The usefulness of this combined system as a tool in magnetic material research will be

demonstrated by means of measurements on Co-Cr films, a promising media for perpendicular recording.<sup>9</sup>

## II. MEASUREMENT SETUP

### A. Introduction

The measurement system of the combined ellipsometer/Kerr loop tracer equipment is based on a polarizer/sample/rotating-analyzer/ellipsometer.<sup>10</sup> A schematic drawing is presented in Fig. 1. As light source ( $L$ ) we normally use a coherent monochromatic HeNe laser (632.8 nm) which can be substituted by a halogen lamp-monochromator combination for wavelength-dependent experiments. Both for the polarizer ( $P$ ) and the analyzer ( $A$ ) we choose a Glan Thompson prism with an extinction ratio<sup>11</sup>  $< 10^{-6}$ . The rotating analyzer ( $A$ ) is speed controlled by means of a tacho (angular frequency 30–100 Hz, accuracy speed control better than 0.05%). The photodiode ( $D$ ) signal is amplified (Amp) to a voltage between 4- and 8-V rms before it is transformed into a numerical series. Discretization and quantization, which are performed by a sample and hold (SH) and an analog/digital convertor (A/D), respectively, are synchronized by a pulse train generated by an optical encoder disk fixed to the axis of the rotating analyzer (128 pulses/revolution). Using the numerical series as input for a discrete Fourier transformation algorithm (DFT) provides us with the Fourier coefficients from which the ellipsometric constants can be easily calculated ( $\Delta$ ,  $\Psi$ , polarization, ellipticity).<sup>12</sup> No analog filters are used to avoid phase errors caused by fluctuations of temperature or rotating analyzer speed. In order to suppress source noise the sampled values can be averaged over several revolutions. By changing this averaging parameter it is possible to exchange measurement time against accuracy. All components can be controlled by a computer so that a high flexibility of the equipment and a high reproducibility of the experiments are guaranteed.

### B. Ellipsometer features

The components of Fig. 1 have been built on two benches which can be rotated through 180° around a sam-

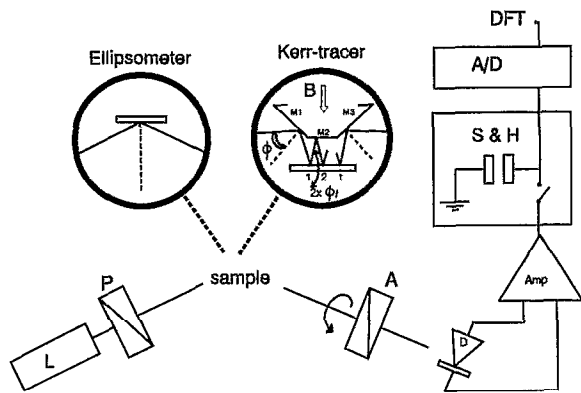


FIG. 1. Schematic diagram ellipsometer/Kerr tracer equipment.

ple holder. Angle-resolved ellipsometry can be performed (angle of incidence can be varied between  $10^\circ$  and  $90 \pm 0.05^\circ$ ).

Although calibration of the  $p$  plane is mostly done by measuring the residue of the detector signal as a function of the polarizer position followed by a determination of the minimum, other procedures can also be applied; phase calibration,<sup>13</sup> Fourier coefficient calibration, and polarization calibration. The  $p$  plane can be found by determining the zeros of the second derivatives of these quantities.

The results presented below were obtained from two zone measurements at  $45^\circ$  and  $-45^\circ$  followed by averaging the ellipsometric data from which the optical properties  $n$  and  $k$  could be automatically calculated. As  $\Delta$  and  $\Psi$  express the ratio between the Fresnel reflection coefficients,<sup>12</sup>  $r_{ss}/r_{pp}$ , the accuracy of this technique becomes worse for smaller angles. With respect to our system the spread in  $n$  and  $k$  measurement values are  $< 0.01$  for an angle of incidence larger than  $50^\circ$ . If the optical benches are not moved throughout the measurement series a spread smaller than 0.001 can be easily obtained.

### C. Kerr loop tracer features

In order to make MO measurements a magnet is placed around the sample. The voltage source of its coil and a Hall probe for measuring the field are both connected to the computer so that the applied field can be automatically controlled. A hysteresis curve can be obtained by varying the field and determining the polarization rotation (accuracy better than  $0.001^\circ$ ).

The software is driven by files which contain macro-commands like "go field", "wait", "measure polarization," etc. (interpreter technique). Besides the standard measurement procedure command files, which are present in the system, the operator can define his or her own measurement procedures so that a high flexibility is guaranteed.

In order to enhance the total field-induced polarization rotation a multiple reflection holder was designed (see inset of Fig. 1).<sup>12</sup> The light beam is reflected several times between a set of mirrors ( $M_1$ ,  $M_2$ , and  $M_3$ ) and the ferromagnetic film. Not only can the quality factor  $R \cdot \theta^2$  of the magneto-optical signal be increased by this configuration

but also the manipulation of the sample between the pole shoes is relaxed. Turning the sample holder around the axis defined by the incoming and outgoing beam makes angle-dependent measurements possible (measurement of the magnetization component normal to the film surface as a function of the magnitude and the direction of the applied field). Beside these advantages the multiple reflection technique also introduces some difficulties. The measured Kerr rotation strongly depends on the state of polarization (SOP) of the incoming beam and the different angles of incidence. This last item demands a very stiff construction of the holder. Beside this stability problem, the reflection with the mirrors will introduce some nonlinearity which has to be kept small or corrected for afterwards. In Sec. II D attention is paid to the design problems of the multiple reflection sample holder.

### D. Multiple reflection sample holder (MRSH)

For the mirrors of the MRSH Ag layers evaporated on silicon with a protection layer of ZrO were used (ellipsometer measurements showed:  $n = 0.025 - 2.10i$ ). This combination guaranteed a high-reflection coefficient which was stable over a period of more than one year.

The (magneto-) optical behavior of the MRSH can be described in terms of Jones matrices.<sup>11</sup> Assume  $J_q(\phi)$  is the Jones matrix for reflection on material  $q$  under an angle of incidence  $\phi$ . The optical transfer function of the MRSH system can easily be calculated from the Jones matrix of each reflection (for the definition of the angles and mirrors see Fig. 1):

$$J_{\text{MRSH}}(\phi, \phi_1, t, M') = J_{\text{Ag}}(\phi) [J_{\text{CoCr}}(\phi_1, M') J_{\text{Ag}}(\phi_1)]^{t-1} \times J_{\text{CoCr}}(\phi_1) J_{\text{Ag}}(\phi) \quad (1)$$

with  $t$  the number of reflections with sample and  $M'$  the relative magnetization  $M/M_s$ .

Excitation of the MRSH with light linearly polarized at an angle  $\alpha$  with the  $s$  plane<sup>12</sup> results in an outgoing beam which can be described by

$$\begin{pmatrix} E_s \\ E_p \end{pmatrix}_{\text{out}} = J_{\text{MRSH}}(\phi, \phi_1, t, M') \begin{pmatrix} \cos(\alpha) \\ \sin(\alpha) \end{pmatrix}. \quad (2)$$

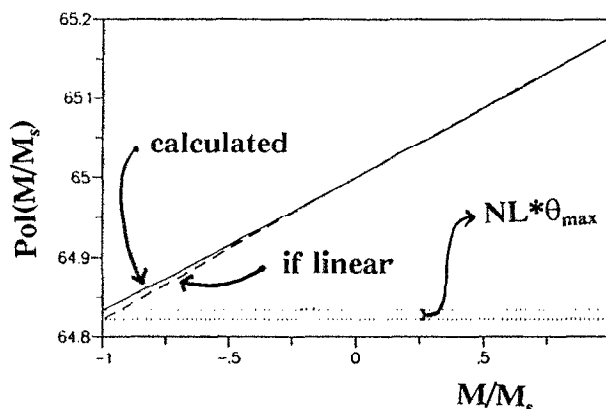


FIG. 2. Calculated polarization as a function of the relative magnetization for a Co film.

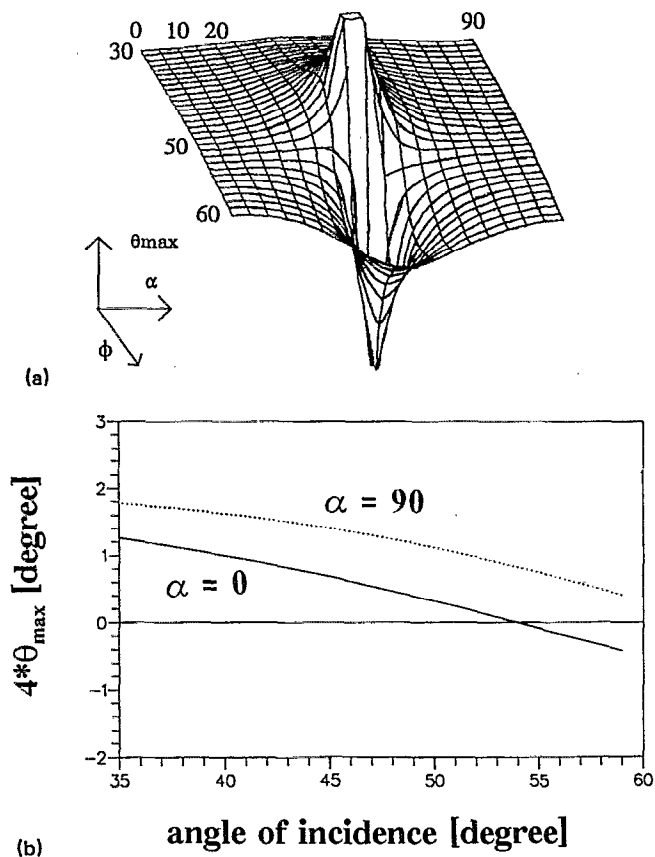


FIG. 3. Calculated polarization rotation for a Co film ( $t = 4, \phi_1 = 0$ ): (a)  $\theta_{\max}(\phi, \alpha)$ ; (b)  $\theta_{\max}(\phi, \alpha)$  and  $\theta_{\max}(\phi, \alpha = 90^\circ)$ .

The polarization direction of this outgoing beam,  $\text{Pol}(M')_{\phi, \phi_1, t, \alpha}$  can be easily found by transforming the vector  $E_{\text{out}}$  to the space defined by the unit vectors RCP and LCP followed by<sup>11</sup>

$$\text{Pol}(M')_{\phi, \phi_1, t, \alpha} = \frac{1}{2} \text{argument} \left[ \frac{E_{\text{LCP}}}{E_{\text{RCP}}} \right], \quad (3)$$

with  $E_{\text{LCP}}$  and  $E_{\text{RCP}}$  the coordinates of  $E_{\text{out}}$  in the LCP RCP space. While  $\alpha$  can be considered as a measurement condition,  $\phi, \phi_1,$  and  $t$  are design parameters which have to be chosen optimally. This optimization can be defined in terms of the next items:

(a) The maximum field induced polarization  $\theta_{\max}$ :

$$\theta_{\max} = \frac{1}{2} [ \text{Pol}(1)_{\phi, \phi_1, t, \alpha} - \text{Pol}(-1)_{\phi, \phi_1, t, \alpha} ]. \quad (4)$$

(b) The nonlinearity (NL) of the magnetic to optic transfer function:

$$\text{NL} = \frac{2 \text{Pol}(0)_{\phi, \phi_1, t, \alpha} - [ \text{Pol}(1)_{\phi, \phi_1, t, \alpha} + \text{Pol}(-1)_{\phi, \phi_1, t, \alpha} ]}{\theta_{\max}}. \quad (5)$$

The meaning of this last quantity is also explained in Fig. 2 where we have plotted the theoretical polarization of the outgoing beam as a function of the relative magnetization of a Co film ( $n = 2.25-4.09i$ ,<sup>14</sup>  $\epsilon_{xy} = 0.41-0.136i$ ,<sup>15</sup> MRS:  $\phi = 60, \phi_1 = 0, t = 4,$  and  $\alpha = 65$ ). As can be seen

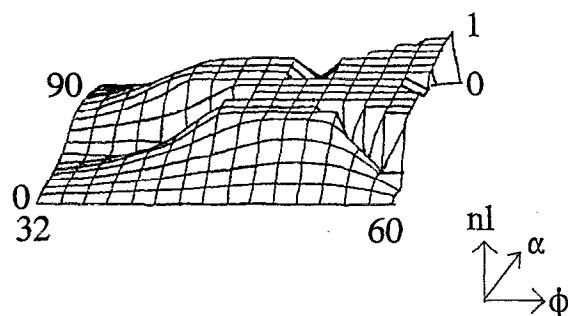


FIG. 4. Calculated nonlinearity for a Co film ( $t = 4, \phi_1 = 0$ ).

from Fig. 2 the relation between observed polarization rotation  $\text{Pol}(M/M_s)$  and relative magnetization  $M/M_s$ , shows a nonlinear relationship. The deviation between this relation and a linear curve is defined as the nonlinearity (NL). We have to choose  $\phi, \phi_1, t,$  and  $\alpha$  so that NL is small and  $\theta_{\max}$  is large.

With Mathcad, a mathematical software package, we calculated  $\theta_{\max}$  as a function of  $\phi$  and  $\alpha$  for Co. The results are shown in the three-dimensional graph of Fig. 3(a). In the horizontal plane the polarization direction  $\alpha$  and the angle of incidence of the incoming beam  $\phi$  are plotted. The height of the surface represents the total field-induced rotation  $\theta_{\max}$ . Figure 3(b) gives a cross section for  $\alpha = 0^\circ$  and  $\alpha = 90^\circ$ . It can be concluded from this graph that the smaller the angle of incidence on the first mirror ( $= \phi$ ) the larger the measured field-induced rotation. Also it can be seen that the field-induced rotation is larger for  $\alpha = 90^\circ$  than for  $\alpha = 0^\circ$ . In the second case the magnetic component (the  $p$ -polarized light) is relatively weakened compared with the optical component (the  $s$ -polarized light) at reflection with mirror 3.

It can also be seen from Fig. 3, that around  $\alpha = 45^\circ$  and  $\phi = 50^\circ$  the field-induced rotation is very high but also very sensitive to changes in  $\phi$  and  $\alpha$ . The influence of small sample movements will result in large signal changes. Figure 4 shows the nonlinearity as a percentage of the total field-induced rotation for several  $\alpha$  and  $\phi$ . The height of the

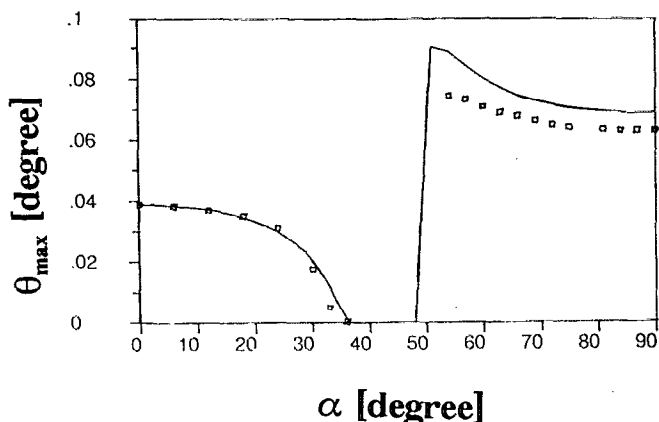


FIG. 5. Measured (squares) and calculated (—) polarization rotation as a function of the polarization of the incoming beam for a Co-Cr film [ $n = 1.85-4.0i, \theta_k - \eta_k = -0.00136 + 0.00035i$  (Refs. 10 and 17)].

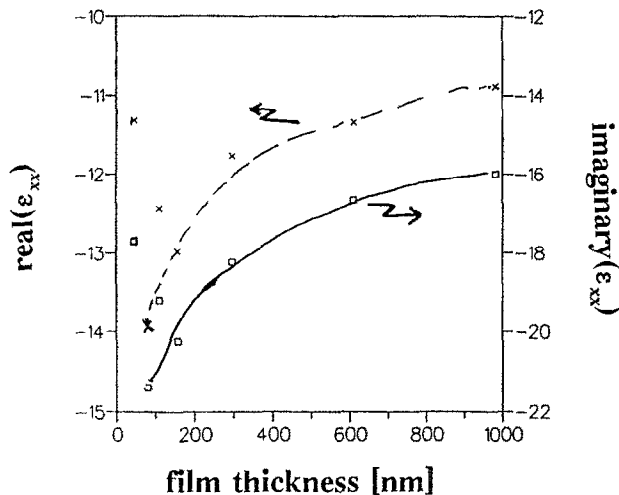


FIG. 6. Optical properties of rf sputtered Co-Cr films as a function of the film thickness.

surface shows the nonlinearity (NL) (nonlinearities larger than 1% are presented as 1%). Choosing 1% as the maximum permitted nonlinearity means that  $\alpha$  must be around  $0^\circ$  or  $90^\circ$ . The calculations above were checked by performing measurements on a Co-Cr film (MRSH:  $\phi = 50 \pm 1$ ,  $\phi_1 = 5$ , and  $t = 4$ ; Co-Cr:  $n = 1.8 - 4.1i$ ,  $\theta_k - \eta_k i = -0.0012 + 0.00035i$ ).<sup>17,18</sup> Using these parameters we also calculated  $\theta_{\max}$  as a function of the polarization rotation of the incoming beam. Results of measurements and calculations are presented in Fig. 5. The differences are most probably due to errors in the values for  $\phi$ ,  $\phi_1$ , and  $n_{\text{Ag}}$  used for the calculations.

### III. MEASUREMENT RESULTS

#### A. Ellipsometric measurements

We measured the optical properties of thin rf sputtered<sup>16</sup> Co-Cr films ( $\lambda = 632$  nm, angle of incidence

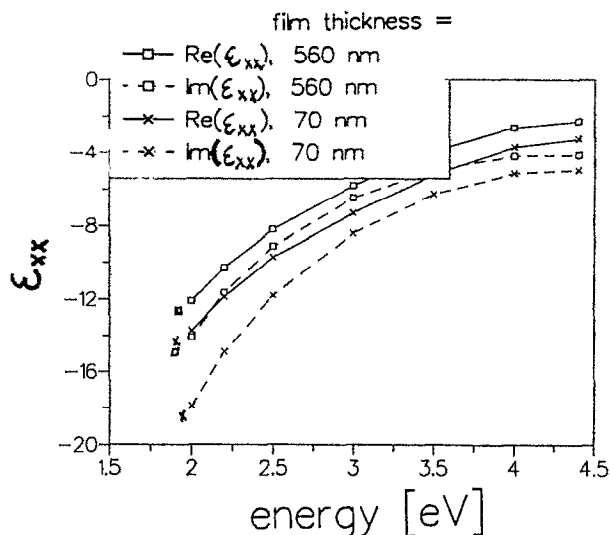


FIG. 7. Wavelength dependence of optical properties for rf sputtered Co-Cr films.

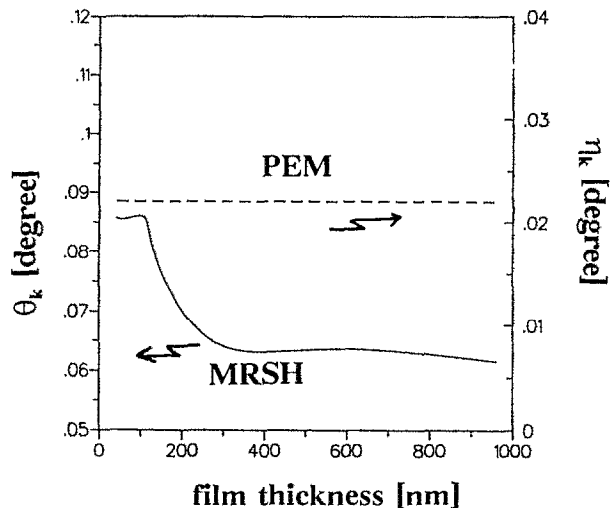


FIG. 8. MO properties of Co-Cr rf sputtered films as functions of the film thickness: (—) Kerr rotation measured by MRSH technique; (---) ellipticity measured by the PEM technique.

$= 70^\circ$ ). Figure 6 shows the real and imaginary parts of  $\epsilon_{xx}$  as functions of the film thickness. Both increase for thinner films. The deviation from the curves for the thinnest film is believed to be caused by multiple reflection (60% penetration depth about 20 nm).

In order to check the performance of our equipment comparable measurements were done with another ellipsometer. The results as a function of the wavelength for a thick (560 nm) and thin (70 nm) Co-Cr film are presented in Fig. 7. Although the experiments were performed at not exactly the same wavelength, extrapolation shows that the results obtained with both measurement systems agree.

#### B. Kerr loop tracer measurements

Using the MRSH technique the Kerr rotation of Co-Cr films as a function of the film thickness was determined<sup>16</sup> ( $\lambda = 632$  nm,  $\phi_1 = 6^\circ$ ,  $\phi = 50^\circ$ ,  $t = 4$ , and  $\alpha = 0$ ). The calibration of the system was done using two Co-Cr films from which the Kerr rotation was known from other experiments. At the Philips Research Laboratories the same

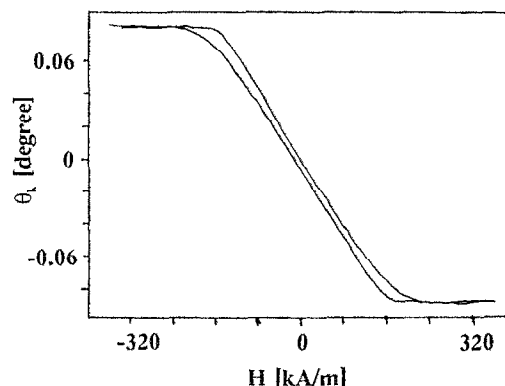


FIG. 9. Typical hysteresis curve measured by multiple-reflection technique.

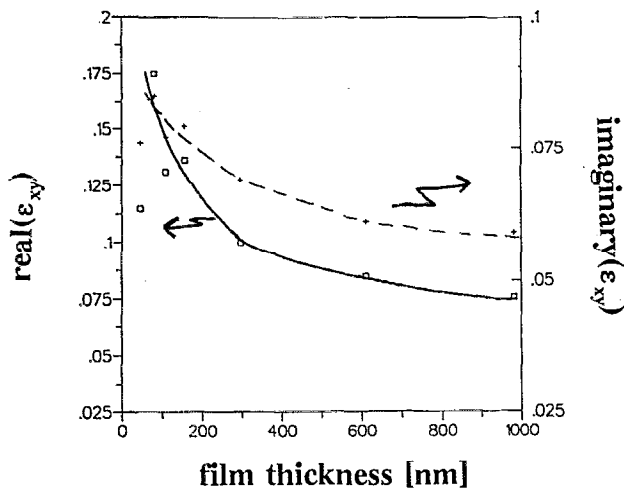


FIG. 10. The off-diagonal components of the dielectric tensor of rf sputtered Co-Cr films as functions of the film thickness.

films were measured using the photoelastic modulator technique.<sup>19</sup> Comparable results were obtained.

The results of ellipticity experiments obtained by this technique are also presented in Fig. 8.

In order to show the accuracy of the system in Fig. 9 the hysteresis curve of a Co-Cr film is plotted. The shape of the curve is similar to that determined by the photo-elastic modulator technique (deviations < 3%).

#### IV. DISCUSSION

Both optical and magneto-optical properties depend on the film thickness. It was found from SEM experiments that the morphology of these films changes as a function of the film thickness.<sup>2,16</sup> The thicker films consist of larger columns and have as a logical consequence a more pronounced roughness. All films were covered with an oxidized top layer of around 6 nm which was almost independent of the film thickness.<sup>3</sup>

As shown in Figs. 6 and 8, the thickness behavior of the optical properties is much more irregular than that of the Kerr rotation. Also  $\epsilon_{xy}$ , calculated from the measurement results, shows this irregular thickness-dependent behavior (see Fig. 10). However it is doubtful if the optical properties measured at 70° by ellipsometry properly describe the reflection at perpendicular incidence. Therefore, the validity of Fig. 10 has to be checked by performing reflection measurements at small angles.

Further we have the impression that the optical properties vary more as a function of their position on the sample than the magneto-optical properties do. Therefore, in order to find the origin of the observed thickness dependency, we have planned to perform combined optical and magneto-optical measurements as a function of the position on the sample.

#### ACKNOWLEDGMENTS

The authors would like to thank Anton Hollink, Rudolf Stammis, Huub Aalbers, Thijs Bolhuis, and Jan van Weers for taking part in the construction of "mechanical," soft, and hardware. The authors also wish to express appreciation to Willie Aarnink of the Solid State group of our university for doing comparable optical experiments and to Dr. W. B. Zeper of the Philips Research Laboratories in Eindhoven for performing PEM measurements on our samples.

- <sup>1</sup>W. Schmitt and A. Eiling, *IEEE Trans. Magn.* **26**, 2131 (1990).
- <sup>2</sup>W. J. M. A. Geerts, J. C. Lodder, and Th. J. A. Popma, paper ICM91, Edinburgh, accepted for publication in *J. Magn. Magn. Mat.*, 1992.
- <sup>3</sup>T. Masuda, W. J. M. A. Geerts, and J. C. Lodder, *J. Magn. Magn. Mat.* **95**, 123 (1991).
- <sup>4</sup>J. Šimšová, J. C. Lodder, J. Kaczér, R. Gemperle, K. Jurck, and I. Tomáš, *J. Magn. Mater.* **73**, 131 (1988).
- <sup>5</sup>J. P. C. Bernards and A. J. den Boef, *IEEE Trans. Magn.* **26**, 1515 (1990).
- <sup>6</sup>R. Allenspach and M. Landolt, *Surf. Sci.* **171**, L479 (1986).
- <sup>7</sup>H. S. Bennet and E. A. Stern, *Phys. Rev. A* **136**, 448 (1965).
- <sup>8</sup>H. Feil and C. Haas, *Phys. Rev. Lett.* **58**, 65 (1987).
- <sup>9</sup>S. B. Luitjens, R. W. de Bie, V. Zieren, J. P. C. Bernards, C. P. G. Schrauwen, and H. A. J. Cramer, *IEEE Trans. Magn.* **24**, 2338 (1988).
- <sup>10</sup>L. J. Hanekamp, W. Lisowski, and G. A. Bootsma, *Surf. Sci.* **118**, 1 (1982).
- <sup>11</sup>A. Nussbaum and R. A. Phillips, *Contemporary Optics for Scientists and Engineers* (Prentice-Hall, Englewood Cliffs, NJ, 1976).
- <sup>12</sup>R. M. A. Azzam and N. M. Bashara, *Ellipsometry and Polarized Light* (North-Holland, Amsterdam, 1977).
- <sup>13</sup>J. M. M. Nijs, A. H. M. Holtslag, A. Hoekstra, and A. van Silfhout, *J. Opt. Soc. Am. A* **5**, 1466 (1988).
- <sup>14</sup>*Handbook of Chemistry and Physics*, 66th ed. (Chemical Rubber, Boca Raton, FL, 1985), p. E376.
- <sup>15</sup>The values of  $\epsilon_{xy}$  of Co reported in literature are scattered. We used the data of Fig. 6 of Ref. 17.
- <sup>16</sup>W. J. M. A. Geerts, J. G. Th te Lintelo, J. C. Lodder, and Th. J. A. Popma, *IEEE Trans. Magn.* **16**, 36 (1990).
- <sup>17</sup>G. S. Krinchik and V. A. Artem'ev, *Sov. Phys. JETP* **26**, 1080 (1968).
- <sup>18</sup>Experimental values of a typical rf sputtered Co-Cr film as determined by ellipsometry (19-at. % Cr).
- <sup>19</sup>J. W. D. Martens, W. L. Peeters, P. Q. L. Nederpel, and M. Erman, *J. Appl. Phys.* **55**, 1100 (1984).